

VHF DISCHARGES IN STORM CELLS PRODUCING MICROBURSTS

P. Laroche, C. Malherbe and A. Bondiou
Office National d'Etudes et de Recherches Aerospatiales
BP 72 92322 Chatillon, Cedex, France

M. Weber, C. Engholm, and V. Coel
Massachusetts Institute of Technology Lincoln Laboratory
Lexington, Massachusetts 02173 USA

1. INTRODUCTION

In the last twenty years, several fatal aircraft accidents have been attributed to encounters with low altitude thunderstorm outflows termed microbursts – outflows which exceed 10 m/s differential velocity over a distance of less than 4 km [1]. The FAA has addressed this issue by establishing the Terminal Doppler Weather Radar (TDWR) program. Under this program, MIT Lincoln Laboratory is sponsored to build a testbed TDWR and test it at various locations in the United States. In the summer of 1990 the testbed TDWR was operationally demonstrated in Orlando, Florida. Research has shown that microbursts are usually associated with convective clouds having high surface rain rates and electrical activity. Williams, et al., [2] and Goodman, et al., [3] have studied these phenomena, both finding that in many cases the peak intra-cloud (IC) lightning flash rate is in phase with the maximum vertical development of the cloud, and that this peak precedes the maximum differential velocity of the microburst by a few minutes. They also found that, in general, IC activity dominates in the early stages of the storm and cloud-to-ground (CG) activity peaks later. In order to confirm and enlarge upon these results, ONERA joined Lincoln Laboratory in Orlando to obtain simultaneous multiple-Doppler and VHF lightning measurements. This paper presents a description and some preliminary results of this joint experiment, including our comparisons of microburst strength and location with the related VHF activity caused by lightning.

2. DESCRIPTION OF THE EXPERIMENT

2.1 The VHF Interferometer

The eventual objective of the joint experiment will be to compare three-dimensional mapping of VHF sources to a three-dimensional description of the reflectivity and dynamics of the associated cloud cells observed by the radar network. Because of scheduling restrictions, we were limited to the use of a two-dimensional interferometer in 1990. The lightning detection equipment installed was a new version of a Systeme d'Alerte Foudre par Interferometrie Radioelectrique (SAFIR) system, designed and marketed by the French firm DIMENSIONS[4]. A SAFIR station is an interferometer with an aerial antenna system which detects a VHF signal, the phase of which is proportional to the azimuth of the emitting source (see figure 1). The VHF signal is processed, digitized, and transmitted by the electronic network installed in a 0.1 m³ box attached to the base of a 17 m high mast supporting the antenna. Data and control signals are transmitted to a central station by a dedicated 9600 baud phone line. VHF locations are displayed in real time at the central station where raw data are stored for off-line analysis. The interferometer is tunable within the international radio navigation band, 110 MHz - 118 MHz. The time resolution of each location is 100 μ s; the acquisition capacity is 100 locations per second. The system used in Orlando consisted of two stations installed 5 km south and 11 km east and west of the TDWR, respectively (see figure 2). The horizontal position of each VHF source is determined by triangulation, yielding an accuracy of better than 1 km within the shaded zone indicated in figure 2. This region encloses the operational area of the TDWR, which includes the airport and its vicinity. For the 1990 experiment, we added an identification device which delivers information on the CG or IC nature of the lightning flash corresponding to the points localized by the interferometer. It is a prototype apparatus based on a wide band measurement of the radiated electric field at ground (5 MHz).

2.2 The 1990 Orlando Radar Network

Detection of microbursts was accomplished using the FAA/Lincoln Laboratory's testbed TDWR [5]. The TDWR is a narrow-beam (0.5°) 5 cm radar. Its signals are processed by algorithms which provide detection of surface outflows of microburst strength, with predictions obtained by utilizing recognition of features aloft. The scan strategy is designed to maximize the algorithms' capabilities, obtaining greater resolution near the surface than aloft. The final output of the algorithms is simple alert information displayed to the air traffic controller (ATC) at the control tower or directly telemetered to the aircraft on a special display installed in the cockpit. Off-line analysis of the radar data is supported by simultaneous 5 cm radar observations taken by the MIT Department of Earth, Atmospheric, and Planetary Sciences radar and the University of North Dakota (UND) radar. These measurements are used for dual- and triple-Doppler analysis to calculate the vertical component of the wind. The update rate is approximately one volume scan every 2.5 minutes, with a surface scan every minute.

3. COMPARISON BETWEEN VHF ACTIVITY AND MICROBURST OCCURRENCE

3.1 Summary of Events Detected by the TDWR

More than 500 microbursts were detected by the TDWR within a range of 70 km of the airport during its operation from early June to mid-September 1990. Most of these microbursts were produced by high reflectivity cells, with precipitation at the ground in excess of 45 dBZ. Figure 3 gives the distribution of the maximum outflow velocity and surface reflectivity. The most frequent value is between 10 and 15 m/s.

3.2 Comparison with VHF Activity

The SAFIR system was in operation from mid-July to mid-September, during which time 123 microbursts were detected within a range of 30 km from the TDWR. The equipment worked well until August 25, but it experienced minor technical problems after that date. The data set of events with both radar and interferometer observations consists of 61 microbursts, most of which were associated with lightning activity. Only two of the events cannot be related to electrical activity: one which gave a weak outflow and another which was produced by a cell with little precipitation (maximum reflectivity of 24 dBZ at the surface). During this same time, 38 large zones of VHF activity were observed, each of which may include several storm cells. Five of these zones exhibited little activity and were not associated with any microbursts. Their activity levels were equivalent to the least active zone which could be associated with a microburst. For this preliminary study, we compared the relative timing and magnitudes of the microburst outflows and the lightning activity. Statistical information about the VHF activity and microburst comparisons are indicated in figure 4. We have considered here only that VHF activity beginning 10 minutes prior to microburst onset or later. This implies that the mean time lags computed are lower than their actual value. From this analysis we note that:

For 93 percent of events, lightning occurred before the onset of the outflow on the ground.
For 65 percent of the cases, the delay exceeds 10 min.

For 77 percent of the events, the first peak in VHF activity occurred up to 10 min before the outflow onset (the mean delay is about 5 min).

For 91 percent of the microbursts, we observed the first peak in activity before the maximum outflow - the mean delay is 9 min.

4. DETAILED ANALYSIS OF MICROBURSTS

In this effort, we wanted not only to confirm past work but also to use the interferometer data to expand in the direction of a more detailed analysis of the structure of individual flashes. We have done this for three different days in August. First we present a review of how flash structure can be inferred from interferometric observations. Following that are an outline of how we define a single flash and its components from a set of VHF sources, a look at the data from the three different days, and two microburst case studies.

4.1 Information Available from the VHF Location System

A lightning flash is composed of a sequence of elementary atmospheric discharge processes. Two different flashes will create different discharge channels. The development of one flash may be directly influenced or initiated by a preceding one (in which case, the two flashes can propagate simultaneously). In general, the time difference between two successive flashes in the same cloud cell is between a few tenths of a second and two seconds. This delay depends on the intensity of the charge separation process. Electromagnetic radiation due to a lightning flash has been measured by several experimenters. Narrow-band measurements were gathered by Pierce [6] and presented on a graph showing normalized magnitude (versus distance and bandwidth) as a function of frequency (figure 5). The form of the resulting curve indicates that the magnitude of the overall radiation is something on the order of $1/f$. The return stroke process involved in the CG flash is mainly responsible for radiation in the low-frequency (LF) and high-frequency (HF) ranges (1 kHz - more than 10 MHz). The VHF radiation, to which our interferometer is sensitive, is mainly due to the pre-breakdown and leader discharges encountered in both CG and IC flashes. The overall duration of a flash is, in general, less than one second. During that time the following phases may be observed:

Pre-breakdown activity occurs up to 200 ms before the onset of a downward negative stepped leader involved in an IC discharge or preceding a return stroke in a CG process. Pre-breakdown activity radiates in HF and VHF ranges [7],[8].

A **stepped leader** is a negative discharge process. It propagates at greater than 10^6 m/s, by steps a few tenths of a meter long. It radiates in the HF and VHF range; steps are fast rise time current pulses of a few kA, which have a repetition rate between $10\ \mu\text{s}$ and $100\ \mu\text{s}$. The typical duration of the propagation of the stepped leader is shorter than 10 ms [9].

A **positive leader** propagates at greater than 10^7 m/s. It constitutes, with the stepped leader (which propagates simultaneously), a neutral and bi-directional discharge process. Its propagation is pulsed, [10] but its current magnitude is low and therefore the radiated energy is very much smaller than that due to the negative stepped leader. The duration of the propagation may be a few hundred ms.

Recoil streamers are high-current IC junction discharges which are hypothesized to propagate within the channel traced by the preceding positive leaders. The velocity of recoil streamers is in excess of 10^7 m/s; [11] peak current measured on an instrumented aircraft may reach 10^5 of kA. This discharge corresponds to the K-change in the electric field [12] which radiates mainly in the VHF range. The duration of a recoil streamer may be as long as $800\ \mu\text{s}$, but the mean duration calculated from a 30-minutes storm observed in southwest France was $150\ \mu\text{s}$. [11]

A **dart leader** initiates the subsequent stroke in a CG flash. It propagates within the channel of the preceding stroke with a velocity of more than 10^7 m/s. Its duration is a few milliseconds and it radiates in the VHF range. [13]

A **return stroke** occurs when a leader connects to ground. It consists of a high-current pulse propagating in the leader channel. Its velocity is up to 10^8 m/s; its magnitude may exceed 100 kA, and its typical duration is less than $100\ \mu\text{s}$.

To understand what kind of analyses are possible with a two-dimensional interferometer system, one must take into account how each of the individual discharge components described above are localized by the apparatus.

Pre-breakdown activity radiates pulsed energy at a rate of one pulse or more each $10\ \mu\text{s}$ over several hundred ms. This activity might not be detected by the system due to the low mean level of emission within a $100\ \mu\text{s}$ time window, or it can be measured as a set of isolated points.

A stepped leader has a low pulse rate emission at the beginning of its propagation (typical stepping rate is $50\ \mu\text{s}$) and again, initially might not be detected by the system. As its propagation continues, the branching of the discharge grows and the mean rate of pulses increases to the point that it becomes detected by the interferometer. Figure 6 shows a plan view of such an event; propagation is detected continuously for 7 ms. Each point might be randomly positioned on the X-Y projection of the propagating front of the discharge. The horizontal extension of the negative stepped leader is small, about 3 km by 3 km for 80 percent of the associated localized points.

Based on results obtained previously with a high-resolution interferometer and on the physical properties of the process, we infer that the radiation due to the positive leader is not normally detected by this kind of equipment.

Recoil streamer and dart leader processes may be associated with the same basic physical process. The associated radiation consists of pulses emitted at a rate of close to or greater than $1\ \mu\text{s}$. With

100 μ s resolution equipment, we observed continuous propagation for a recoil streamer, the duration of which exceeded 100 μ s. Figure 7 shows the horizontal projection of a flash exhibiting several recoil streamers.

VHF radiation emitted by return strokes is weaker than its LF counterpart. We know from previous measurements that the magnitude of the VHF radiation is great enough to be localized by our equipment.

4.2 Criteria Applied for the Analysis of Lightning Phenomenology

We have used the understanding related above to formulate automated algorithms for identifying flashes, recoil streamer or dart leaders, and negative leaders. The following two criteria were used to determine if a set of points belong to a single flash:

1) The overall duration of a flash must be less than or equal to one second.

2) Two successive points in a flash are separated by a horizontal distance of no more than 25 km, or a distance equivalent to a horizontal velocity of no more than $5 \cdot 10^7$ m/s.

Within a single flash, a recoil streamer or dart leader processes is identified as a burst of points with the following two characteristics:

1) We require a burst to be composed of at least two locations, even though previous measurements demonstrate that the mean recoil streamer duration may be less than 200 μ s.

2) The points within a burst may not be separated by more than 200 μ s (two successive samples where VHF activity is below threshold). This allows for any lack of sensitivity in the VHF receiver.

A negative leader is identified by a burst of at least 10 points. We note that our data indicate that the burst associated with a negative leader exhibits small horizontal extent.

4.3 General Activity Associated with Three Different Storm Days

Having identified flashes and their components, we chose three days with microburst activity on which to concentrate our analysis. We analyzed the VHF locations observed within an area limited to about 70 km east and west and up to 80 km north of the TDWR. The beginning and ending times of the period processed were approximately 10 minutes before the first surface outflow differential velocity reached 10 m/s and 10 minutes after the last outflow fell below 10 m/s. In table 1 below we indicate the overall number of locations, flashes, bursts, and leaders for time periods from August 16, 18, and 22. Due to a technical problem, August 18th is divided into in two sequences, separated by 7 minutes without VHF information.

Table 1. Analysis of VHF activity for three storm days.

Date	Time (min)	Num. of points		Num. of Flashes		Num. of Bursts		Num. of Leaders	Bursts/Flash	% Flashes with a Leader
		total	per min	total	per min	total	per min			
8-16	87	9162	105	811	9.3	1557	17.9	84	1.90	10.3
8-18 I	36	2920	81	756	21.0	514	14.3	4	0.68	0.5
II	59	6375	108	600	10.2	1017	17.2	77	1.69	12.8
total	95	9295	97	1356	14.3	1531	16.1	81	1.13	6.0
8-22	88	9222	105	1421	16.1	1739	19.8	59	1.22	4.2

For August 16, we observed a mean flash rate of 9.3 flashes per minute, with 10.3 percent of these flashes containing a recognizable leader. This is the lowest flash rate for any of the three sequences, but a relatively large percentage of flashes with negative leader detection.

The first part of the sequence from August 18 corresponds to the onset of general activity. We observed a high mean flash rate (21 flashes per minute) and the lowest percentage of flashes with leader detections (0.53 percent); it must be pointed out that a large number of these flashes are identified by a single point. It should also be noted that past work (e.g. Williams, et al.[2]) suggests that the onset of activity is likely to contain fewer CG flashes, i.e., fewer negative leaders. The second part of the sequence is similar to August 16: 10.2 flashes per minute and 12.8 percent of which contain a recognizable leader. Combining the two sequences we see flash rate and leader detection percentages that lie between the values computed for the other two storm days.

For the sequence from August 22, we observed a higher mean flash rate (16.1 flashes per minute) and a lower rate of leader detection (4.15 percent of the flashes) compared to the other two storm days. To summarize, we note that:

1) The mean detection rate is basically the same for the hour and a half duration of the sequences (105 locations per minute), except for the first part of August 18 during which the rate is lower (81 locations per minute).

2) The mean rate of burst identification is consistent between three of the sequences (about 18 bursts per minute). The exception is the first sequence of August 18, whose identification rate is lower in the same proportion as the mean location rate (about 14 bursts per minute; that is, 30 percent less than that observed in the other cases).

3) The three similar sequences (August 16, August 18 II, and August 22) exhibit different flash rates and different percentages of flashes with a negative leader detection.

4.4 Case of Microburst #6 (MB6) of August 16

Six outflows were identified by the TDWR on August 16, 1990. Each outflow is identified by its type (e.g., microburst (MB)) and an event number. The outflow corresponding to MB6 was first identified by the TDWR at 22h57. A maximum outflow differential velocity of 24 m/s was reached at 23h06, and the differential velocity dropped back below the 10 m/s threshold at 23h19. During the 22 minutes of the outflow, its location changed less than 3 km east-west from its mean position of 29 km north and 11 km east of the radar.

This microburst position corresponded to the large area of VHF activity represented in figure 8a. The overall evaluation of the activity in this electrical cell between 22h45 and 23h11, which is the time interval corresponding to the most active phase, is characterized by the following:

4720 VHF sources detected (181 sources/min)

463 flashes (17.8 flashes/min)

826 bursts (31.7 bursts/min)

36 negative leader detections (7.8 percent of all flashes had a leader detected)

This activity was much greater than the mean general activity observed on the same day (described in table 1 above). This one cell contained over half of all the VHF detections, flashes, and burst detections of that day. The percentage of flashes with leader detections was slightly less than the mean - 7.8 compared to 10.3 percent.

The boundary of the electrical cell associated with this microburst is stationary. The 40 dBZ surface reflectivity contour, which was used to define the cloud cell, moves slightly northward. At the beginning of the outflow, the precipitation was south of the electrical activity, although the correlation between both phenomena is quite good at the end of the life of the microburst.

A comparison of the electrical and cloud cells indicates that the VHF activity clearly preceded the collapse of the cloud cell.

The relative evolutions of the electrical and cloud activity can also be seen through a comparison between flash rates and outflow strength. Figure 8b indicates the temporal evolution of the total flash rate, leader detection rate, and CG flash rate indicated by the flash identification algorithm. We have also drawn the time evolution of the outflow on the same figure. We note a rather good qualitative correlation between leader rate detection and CG flash rate. This supports the idea that negative

leaders may be involved in a CG process.

Peak IC activity was reached at 22h54; peak CG activity was reached one minute later. Absolute peak activity happened at 22h58, with a value of 34 flashes/min. This very high flash rate is evidence that this electrical activity is not associated with a single dynamic cell, but more likely with a set of several active centers. A peak flash rate of 10 flashes per minute is what is commonly observed at other sites.

We observe a regular increase in the number of bursts per flash and of the mean burst duration (up to 8 per flash and 600 μ s duration around 23h). The distribution of the mean horizontal velocity of each burst indicates a peak frequency between 2 and 5 $\cdot 10^7$ m/s. The distribution of time intervals between successive bursts shows three peaks of frequency:

1.8 percent between 1 and 3 ms;

12.0 percent between 10 and 30 ms; and

13.3 percent between 100 and 300 ms.

The overall peak frequency is 10.2 percent for the 100-200 ms interval. This point is discussed more fully in Section 5.

There is one further interesting point to note about the negative leaders and their relationship to the microburst outflow. The leader horizontal development is limited to a region which is approximately 5 km in diameter, and the mean position of leaders remains close to the microburst location (see figure 8a).

4.5 Case of Microburst #5 (MB5) of August 16

The outflow corresponding to MB5 develops southwest of MB6, from 23h12 to 23h31. A maximum outflow velocity of 20 m/s is reached at 23h17. VHF activity is observed in the vicinity of MB5 between 22h31 to 23h28. This activity was very much weaker than the mean general activity observed:

1402 locations (24.6 locations/min — 1/4 the mean rate)

101 flashes (1.8 flashes/min — 1/5 the mean rate)

239 bursts (4.2 bursts/min — 1/4 the mean rate)

12 negative leaders observed by the interferometer (11.9 percent of all the flashes — similar to the mean rate)

A heavy precipitation area at the surface corresponded to an area of horizontal VHF activity, but the relative maximum of both phenomena are not coincident. Still, the development of the negative leaders are mainly in the vicinity of the outflow (see figure 9).

The first peak in IC activity is reached at 23h05 (7 minutes before the onset of the outflow). The peak CG activity is reached at 23h13 (figure 9). The number of bursts per flash, the mean burst duration, and the mean flash duration increase regularly up to the end of the life of the electrical cell (with maximums of 4 bursts per flash, 400 μ s burst duration, and 0.9 s flash duration). The distribution of the mean horizontal velocity of the bursts shows a maximum frequency between 5 $\cdot 10^6$ and 10⁷ m/s. The distribution of time intervals between successive bursts presents the same characteristics as for the case of MB6 — i.e., three local maxima of frequency are observed:

6.7 percent between 1 and 3 ms;

15.5 percent between 10 and 30 ms; and

11.3 percent between 100 and 300 ms.

The overall peak frequency is 10 percent between 100 and 200 ms. Except for intervals 1-3 ms, these values are close to those obtained for MB6, and are discussed below.

5. DISCUSSION

A preliminary overview of the data available for 61 cases of microbursts shows clearly, in 93 percent of the cases, that the electrical activity precedes the development of outflow. Our results strongly confirm the results of Williams, et al.,[2] and Goodman, et al.,[3] that the peak in IC activity precedes the maximum value of the outflow. We find this same result in 91 percent of the events. For several cases, we observed a correlation between the onset of the IC electrical activity and the development of slantwise divergence at mid and upper levels (i.e., divergence along PPI's at altitudes of 7 km and above). The presence of this signature may suggest an updraft at these levels, but both the interpretation of this feature and its relationship to electrical activity has yet to be confirmed by more extensive analysis.

We have not yet found any direct relationships between the magnitude of the outflow and the intensity of the corresponding electrical activity. The two examples presented above illustrate this point clearly. We are continuing our work in this area.

The analysis of VHF activity due to atmospheric discharges derived from a limited time resolution two-dimensional interferometer (100 μ s - 100 locations per second) give valuable information on the behavior of the lightning flash. The interferometer detected the strongest and closest negative stepped leader processes. We have verified that the ratio of flashes with leader detection increases when the storms are closer to the measuring stations. Temporal comparison with a return stroke identification system confirms that these leaders are associated with CG processes preceding return strokes. This comparison is, up to now, qualitative due to some technical problems which can be resolved by a more elaborate data reduction process.

Observed burst propagations are known to be due to recoil streamers or dart leader processes [9]. The distribution of velocity of such phenomena obtained with a high-resolution three-dimensional interferometer indicated a mean velocity of $2 \cdot 10^7$ m/s for a set of 800 bursts detected during 20 minutes of a storm in southwest France. These results are consistent with those presented here for Florida storms. Even if the actual distribution may be centered on a slightly lower velocity (for example, 10^7 m/s for MB5), this means that the propagations are mainly horizontal. This supports the results by Krehbiel [14] which indicated that the propagation of positive leaders (in channels in which recoil streamers are supposed to propagate) has an important horizontal component.

The distribution of time intervals between successive bursts contains, for most of the cases we observed, three peaks. The first one (1 to 3 ms) is typical of that observed for M-changes and, in that case, can be associated with a continuing process (which corresponds to the propagation of a positive discharge) [15]. The second one (10 to 30 ms) corresponds to the mean interval between successive recoil streamers[16]. The third peak (100- 200 ms) might correspond to a dart leader preceding the return stroke process. This point may be inferred from statistical results showing that in the vicinity of Kennedy Space Center (KSC), the mean interval between strokes of natural flashes is 86 ms,[17] the same as for all the flashes triggered at KSC by the wire and rocket technique between 1984 and 1989. For those two experiments, it has been shown that the mean number of strokes per flash is between two and three. The ratio between the number of leaders and bursts of this last category is quite consistent with that point.

The objectives of our work are to find, within the temporal and spatial characteristics of IC and CG lightning activity, information to predict, with good reliability, the place and time of microburst events. In order to achieve this goal, we will be continuing our analyses by:

- 1) Extensively comparing the VHF activity with information on cloud features present in the radar data above the surface layer, and
- 2) Conducting a similar experiment with a three-dimensional interferometer to relate the electrical activity to the vertical development of the cell.

ACKNOWLEDGMENTS

This work has been done under contracts of DRET (French DOD) and DGAC (French civil aviation authority). Collaborative experiments involving MIT and ONERA have been organized via a DEA between the FAA and DGAC. The work of MIT Lincoln Laboratory is sponsored by the FAA.

References

- [1] T.T. Fujita and F. Caracena, An analysis of the weather related aircraft accidents, Bull. Amer. Met. Soc., 1977, vol. 58, pp 1164-1181.
- [2] E. Williams, M.E. Weber, and R. Orville, The relationship between lightning type and convective state of thunderclouds, Int. Conf. on Atmos. Elec., Uppsala, Sweden, 1988.
- [3] S. Goodman, E. Bueckler, and D. Wright, Lightning and precipitation history of a microburst producing storm, GR Letter, vol. 15 no. 11, pp. 1185-1188.
- [4] P. Richard, SAFIR system, an application of real time VHF lightning location to thunderstorm monitoring, Sixth Conf. on Severe Local Storms, American Meteorological Society, Canada, October 1990.
- [5] M. Merritt, D. Klinge, J.W. Wilson, and S.D. Campbell, Windshear detection with pencil beam radars, Lincoln Laboratory Journal, vol. 2, no. 3, pp. 483-510.
- [6] E.T. Pierce, Atmospheric and radio noise, in lighting, edited by R.H. Golde Academic Press Inc., London, 1977.
- [7] P. Richard, A. Delannoy, G. Labaune, et P. Laroche, Results of spatial and temporal characterization of the VHF-UHF radiation of lightning, JGR, vol. 91, no. D1, January 20, 1986.
- [8] W.H. Beasley, M.A. Uman and P.L. Rustan, Electric fields preceeding cloud to ground lightning flashes, JGR, vol. 86, 1982.
- [9] E.P. Krider and G. J. Radda, Radiation field wave forms produced by lightning stepped leaders, JGR, vol. 80, no. 18, June 1975.
- [10] P. Laroche, A. Eybert-Berard, L. Barret, and J.P. Berlandis, Observations of preliminary discharges initiating flashes triggered by the rocket and wire technique, Eighth Int. Conf. on Atmos. Electricity, Uppsala, Sweden, June 1988.
- [11] A. Bondiou, I. Taudiere, P. Richard, and F. Helloco, Analyse spatio-temporelle du rayonnement VHF-UHF associe a l'eclair, Revue de Physique Appliquee, no. 25, February 1990, pp. 147-157.
- [12] N. Kitagawa and M. Kobayashi, Field changes and variations of luminosity due to lightning flashes, in Recent Advances in Atmospheric Electricity, L.G. Smith Pergamon Press, 1959.
- [13] P. Richard, A. Delannoy, G. Labaune, et P. Laroche, Results of spatial and temporal characterization of the VHF-UHF radiation of lightning, JGR, vol. 91, no. D1, January 20, 1986.
- [14] P. Krehbiel, M. Brook, and R.A. McCrory, An analysis of charge structure of lightning discharges to ground, JGR vol. 84, pp. 2432-2456, 1979.

[15] R. Thottappillil, V.A. Rakov, and M.A. Uman, K and M changes in close lightning ground flashes in Florida, JGR, vol. 95, no. D11, October 1990.

[16] N. Kitagawa and M. Kobayashi, Field changes and variations of luminosity due to lightning flashes, in Recent Advances in Atmospheric Electricity, L.G. Smith Pergamon Press, 1959.

[17] R.D. Brantley, J.A. Tiller, and M.A. Uman, Lightning properties in Florida thunderstorms from video tape records, JGR, vol. 80, no. 24, August 1975.

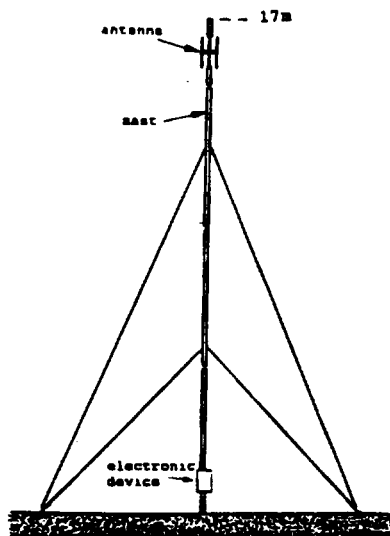


Figure 1: VHF interferometer measuring station.

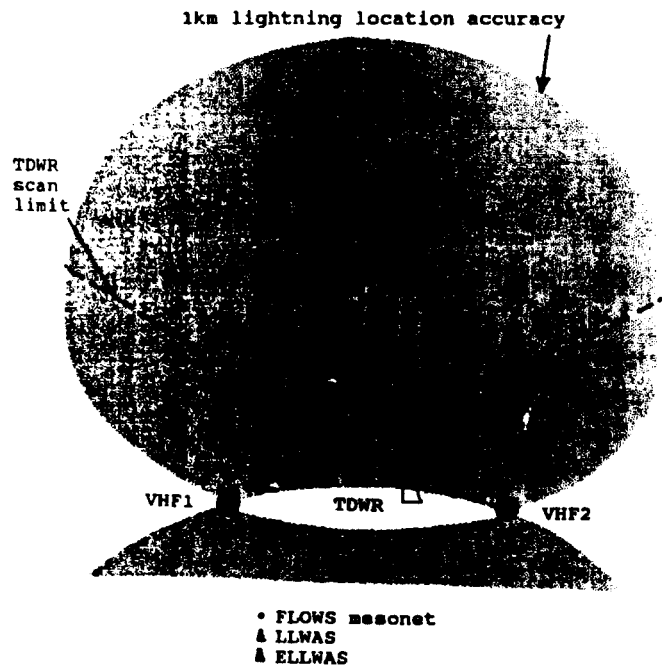


Figure 2: Orlando 90 network.

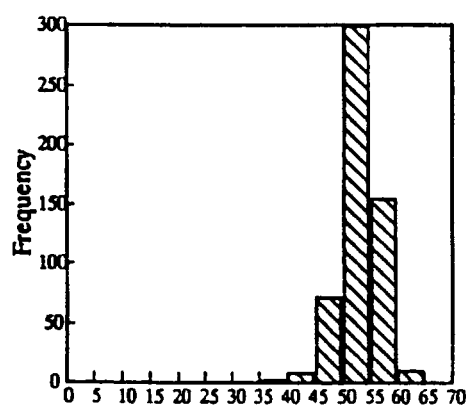
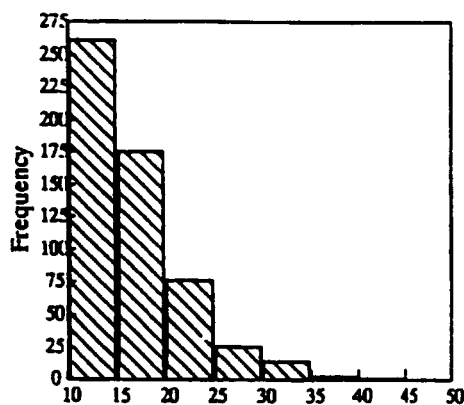


Figure 3: Distribution of outflow strength and surface precipitation for the more than 500 microburst cases detected during operations in Orlando, Florida.

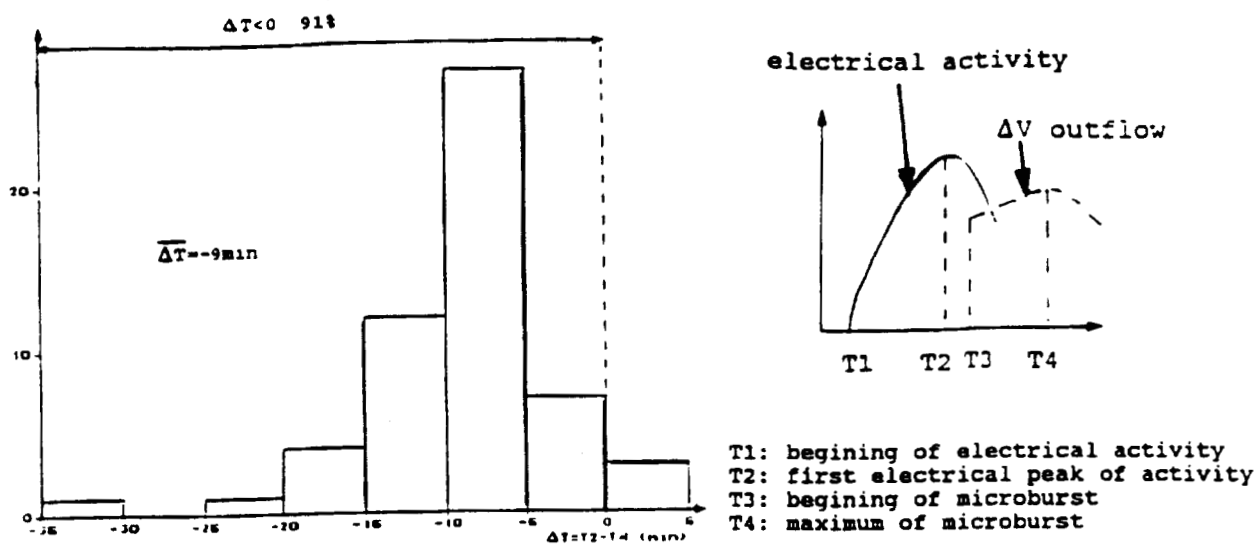


Figure 4: Statistical comparisons between VHF activity and microburst development.

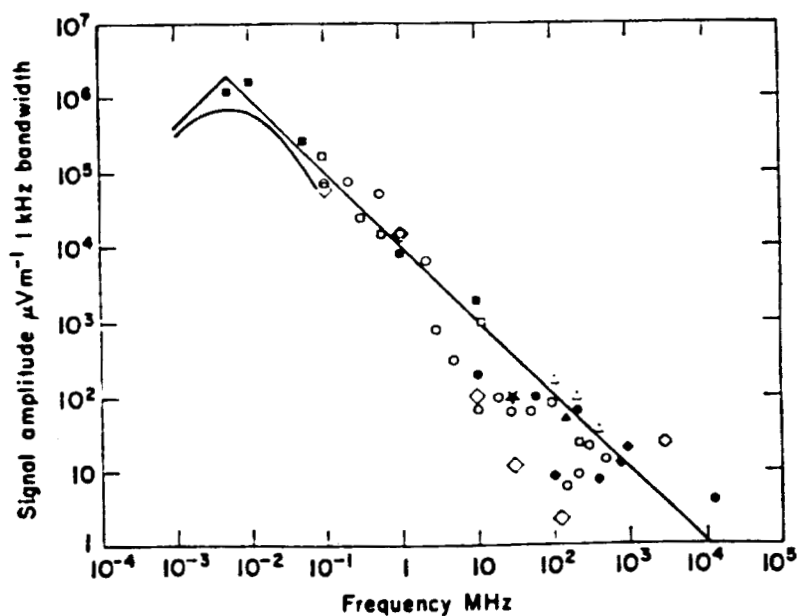


Figure 5: Peak received amplitude at 10 km for signals radiated by lightning (E.T. Pierce).

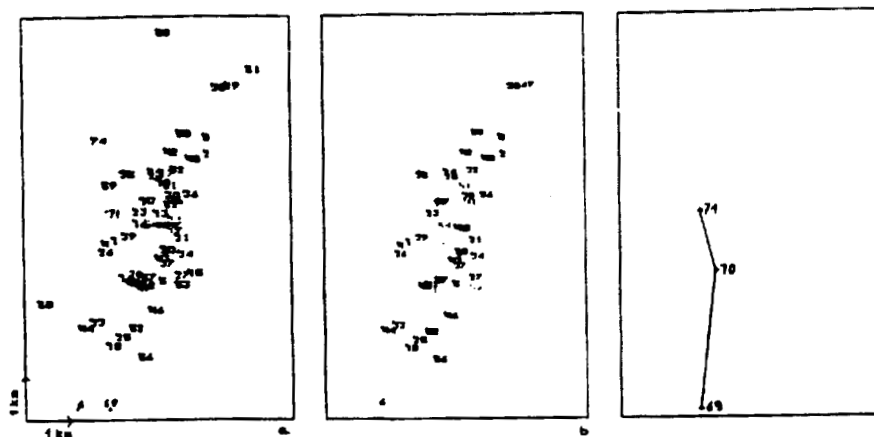


Figure 6: Flash initiated by a negative step leader. The overall horizontal flash extension is 8,7km x 5km but, 80% of the locations are included in a 2,8km x 3,3km. This event is made of 74 locations, it lasts 137,5 ms (a). The first event is a negative leader of about 7 ms duration (b) which is followed by 5 bursts (recoil-streamer or dart leader) at time intervals between 14 ms and 60 ms. One of those bursts is presented on figure c. It lasts 300 μ s.

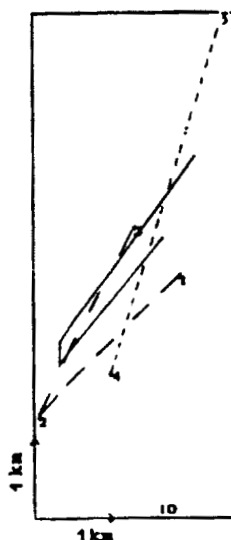
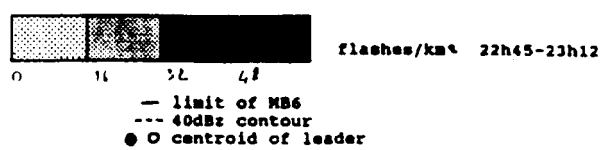
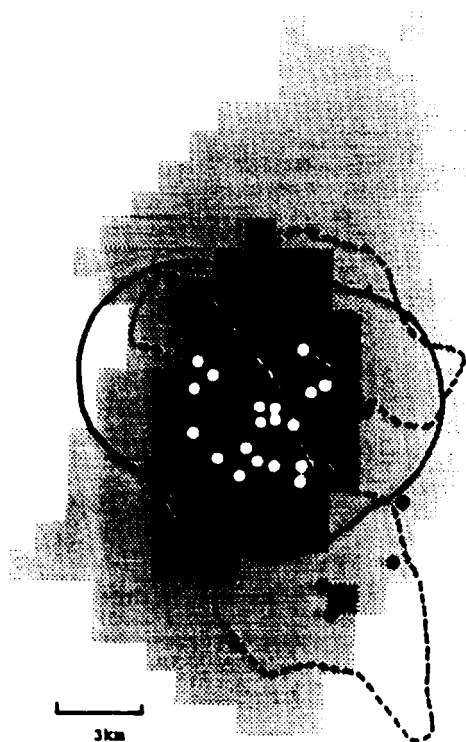
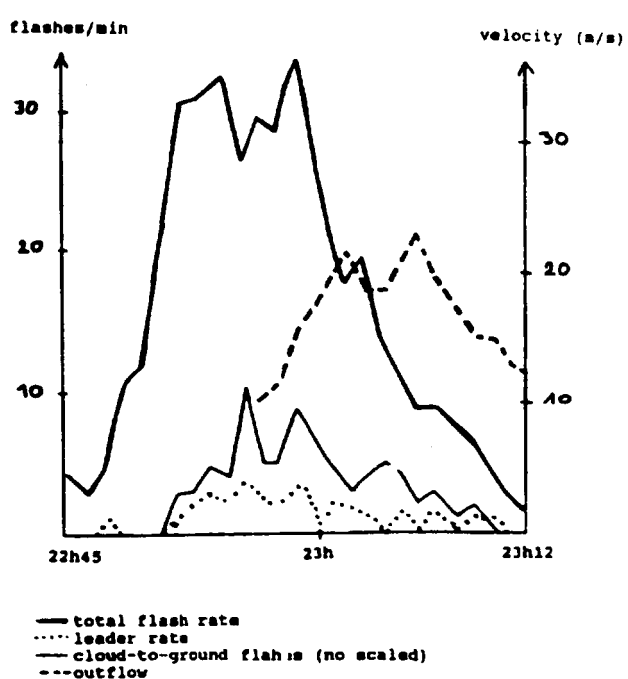


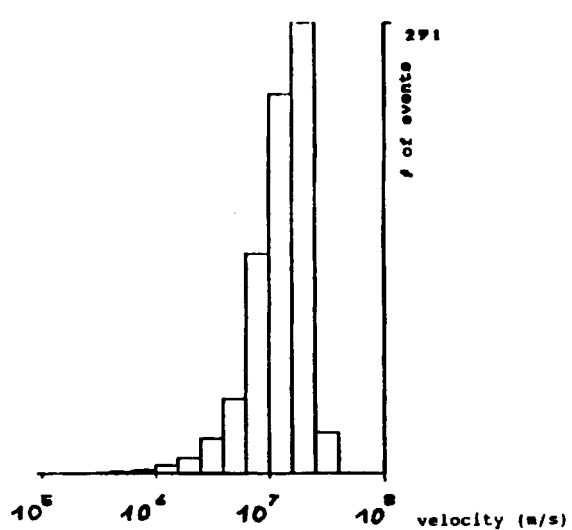
Figure 7: Intra-cloud flash with 3 bursts. The flash is made of 10 locations. Its duration is 345,3 ms. Its overall extension is 2,5km by 6km.



a: Location of microburst, 40dBz reflectivity and VHF activity. 22h45-23h12

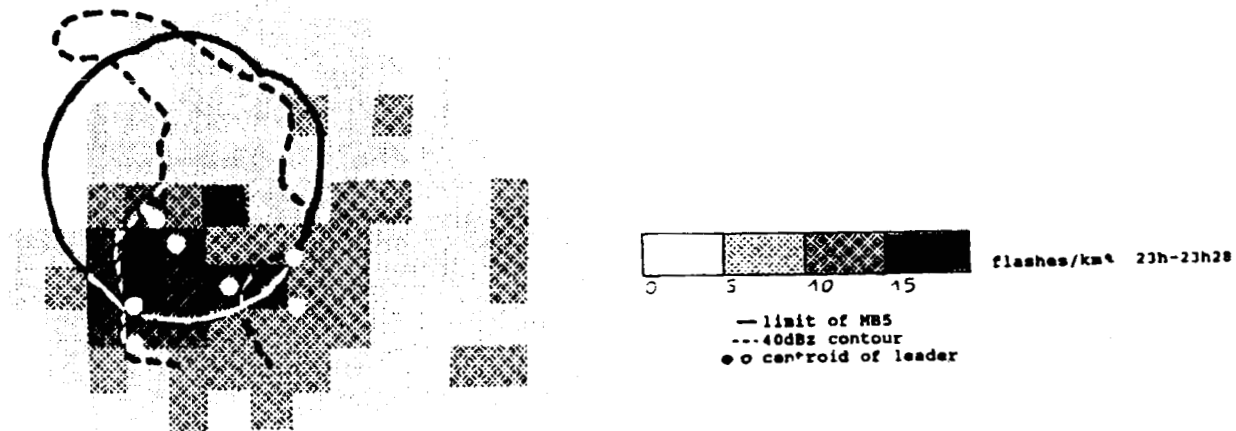


b: Temporal evolution of flashes rate and microburst development

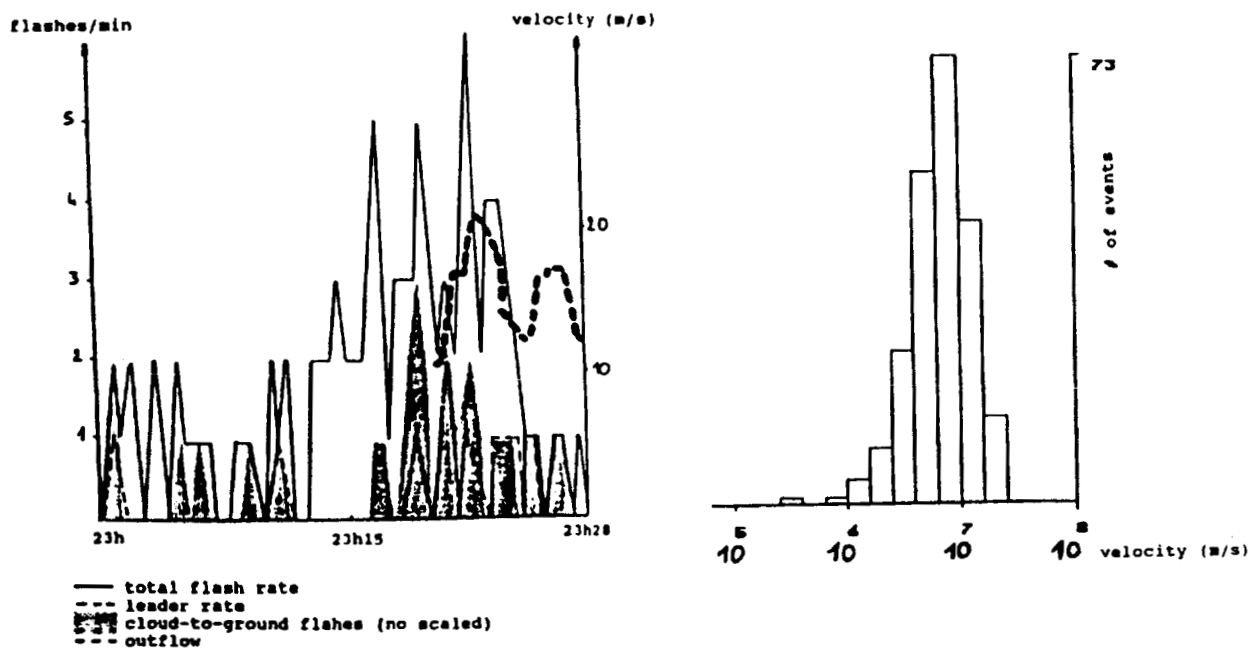


c: Bursts mean velocity distribution

Figure 8: Case of microburst #6 of August 16.



a: Location of microburst, 40dBz reflectivity and VHF activity. 23h-23h28



b: Temporal evolution of flashes rate and microburst development

c: Bursts mean velocity distribution

Figure 9: Case of microburst #5 of August 16.